Anal Bioanal Chem (2003) 377 : 578–586
DOI 10.1007/s00216-003-2080-1

ORIGINAL PAPER

**Carine Galli Marxer · Martine Collaud Coen
Thomas Greber · Urs F. Greber · Louis Schlapbach**

Cell spreading on quartz crystal microbalance elicits positive frequency shifts indicative of viscosity changes

Received: 11 March 2003 / Revised: 1 May 2003 / Accepted: 20 May 2003 / Published online: 19 July 2003

Abstract Cell attachment and spreading on solid surfaces was investigated with a home-made quartz crystal microbalance (QCM), which measures the frequency, the transient decay time constant and the maximal oscillation amplitude. Initial interactions of the adsorbing cells with the QCM mainly induced a decrease of the frequency, coincident with mass adsorption. After about 80 min, the frequency increased continuously and after several hours exceeded the initial frequency measured before cell adsorption. Phase contrast and fluorescence microscopy indicated that the cells were firmly attached to the quartz surface during the frequency increase. The measurements of the maximal oscillation amplitude and the transient decay time constant revealed changes of viscoelastic properties at the QCM surface. An important fraction of these changes was likely due to alterations of cytosolic viscosity, as suggested by treatments of the attached cells with agents affecting the actin and microtubule cytoskeleton. Our results show that viscosity variations of cells can affect the resonance frequency of QCM in the absence of apparent cell desorption. The simultaneous measurements of the maximal oscillation amplitude, the transient decay time constant and the resonance frequency allow an analysis of cell adsorption to solid substratum in real time and complement cell biological methods.

C. Galli Marxer (✉) · M. Collaud Coen · L. Schlapbach
Solid State Physics Research Group, University of Fribourg,
Pérolles, 1700 Fribourg, Switzerland
e-mail: Carine.Galli@unifr.ch

T. Greber
Institute of Physics, University of Zürich,
Winterthurerstrasse 190, 8057 Zürich, Switzerland

U. F. Greber
Institute of Zoology, University of Zürich,
Winterthurerstrasse 190, 8057 Zürich, Switzerland

L. Schlapbach
Swiss Federal Laboratories for Materials Testing and Research,
Ueberlandstr. 129, 8600 Dübendorf, Switzerland

Keywords Cell · QCM · Adsorption · Cytoskeleton · Amplitude · Decay time constant

Introduction

The shape and the mechanical properties of a cell are largely controlled by the cytoskeleton and the underlying regulatory circuits (reviewed in [1, 2, 3]). The cytoskeleton and associated proteins critically influence basic cell functions, including growth, motility, apoptosis, and differentiation [4, 5], and also resistance towards deformation [6, 7]. A variety of methods are available to study the mechanical properties of the cytoskeleton. Light microscopy provides images of the dynamic shape of both, living and chemically fixed cells in time and space [8, 9]. Magnetic twisting cytometry measures the rotation of magnetic particles in contact with the cell membrane and serves to determine the cytoplasmic viscosity and consistency [10, 11, 12, 13]. Magnetic bead microrheometry gives similar information by measuring the position of the particles [14, 15, 16]. Additional methods to measure contractile forces include pulling of adsorbed cells with a needle [17], micropipette aspiration of cells [18, 19, 20, 21], or directly poking cells [22, 23]. A major disadvantage of these methods is that they are invasive. In contrast, the quartz crystal microbalance (QCM) allows non-invasive measurements of mass adsorption and biophysical changes on defined substrata [24].

The QCM has been developed to measure molecular adsorption under vacuum [25, 26]. In this case the measured resonance frequency shift of an oscillating quartz is linearly proportional to the adsorbed mass according to the Sauerbrey equation [27]. The QCM was further developed to study adsorption in liquids [28]. This required to determine the mass-induced frequency shift and additional physical properties, such as the density and viscosity of liquid [29]. When the quartz vibrates at its resonance frequency and is immersed into a fluid, an exponentially damped wave is coupled into the liquid. With 10-MHz quartz crystals under water loading at 37 °C the

penetration depth is about 180 nm. It is therefore possible to detect in real time phenomena occurring at the interface of the electrode surface and living matter, such as single cells or tissues. More precisely, the processes of cell attachment and spreading and the underlying modifications of the mechanical properties can be analyzed.

Previous experiments with cultured cells have measured the frequency f and the resistance using a steady state technique [30, 31, 32, 33] or have measured f and the dissipation factor D [34, 35, 36] using a transient technique. We have recently developed a QCM device based on a transient technique, which detects mass and viscoelasticity changes in real time by periodically interrupting the quartz excitation and measuring the resonance frequency (f), the transient decay time constant (τ), and the maximal oscillation amplitude (A_0) [37].

Here we report that the resonance frequency decreased during 60–80 min of cell attachment to the QCM surface. Thereafter, positive frequency shifts were measured. The maximal amplitude A_0 and the transient decay time constant τ indicated that cell desorption did not occur during this phase and this was independently confirmed by light microscopy. The readout of f, A_0, and τ indicated an increased rigidification of cells during the spreading process, and this was verified by changing cell viscosity using microtubule- and actin-directed drugs.

Materials and methods

Cells

TC7 African Green Monkey kidney epithelial cells and HeLa cells (American Type Culture Collection) were grown on plastic dishes in a humidified 5% CO_2 air atmosphere at 37 °C in Dulbecco's Modified Eagle's Medium (DMEM) (Gibco) containing 10% Fetal Calf Serum (FCS) (Hyclone) and 2 mM L-glutamine as described earlier [38]. A549 (lung carcinoma) cells were grown in similar conditions in DMEM (Gibco) containing 7% Clone III (Hyclone) and 2 mM glutamine. Near confluency cells were detached from the substrate by short treatment with trypsin (0.5 mg mL^{-1}) at 37 °C and immediately resuspended in RPMI medium (Gibco) supplemented with 20 mM Hepes and 10% FBS (TC7 and HeLa) or 7% Clone III (A549), 2 mM glutamine, 1% nonessential amino acids, 100 U mL^{-1} penicillin/0.1 mg mL^{-1} streptomycin. The cells were then immediately transferred to the QCM.

Drugs

Different drugs were used to disturb the polymerization state of actin filaments and microtubules of spread out cells on the quartz crystal. The drugs were dissolved in dimethylsulfoxide (DMSO) and diluted in the media lacking cells at 1:1000. Jasplakinolide (Jas) (a gift from Phil Crews, Santa Cruz, California) induces actin polymerization and competes with phalloidin for actin binding [39, 40, 41]. It was used at a concentration of 500 nM [42]. Latrunculin B (LatB) (Calbiochem, Juro Supply), which was used at a concentration of 1 µM, forms 1:1 complexes with actin monomers and inhibits actin polymerization [43, 44]. Cytochalasin D (CD) (Calbiochem, Juro Supply) binds to the faster-growing end of actin [45] and disrupts the filaments [46]. The concentration of CD was 2 µM. Microtubule polymerization was induced by Paclitaxel (Taxol) (Sigma) 2 µM [47] and microtubule depolymerization was induced by Nocodazole (Noc) (Sigma) 20 µM.

Quartz crystal microbalance (QCM)

The sensor of the QCM consists of a thin quartz plate with two Au-evaporated electrodes on each side. 10-MHz AT-cut crystals with an active sensor area of 20 mm^2 were from Internal Crystal Manufacturing Co, Inc, OK, USA. The application of an alternative voltage with a frequency near the quartz resonance frequency induces oscillation of the quartz at its resonance frequency. Under vacuum a change of resonance frequency Δf is proportional to the amount of adsorbed mass Δm according to the Sauerbrey relation [27]:

$$\Delta m = -C \cdot \Delta f$$

where C represents the quartz sensitivity, which is 4.5 ng/Hz cm^2 for our 10-MHz crystals. Under liquid loading an additional frequency shift arises, which is proportional to the liquid density ρ_l and viscosity η_l (Kanazawa's equation) [29]:

$$\Delta f = -f_0^{3/2}\sqrt{\frac{\rho_l \eta_l}{\pi \mu_q \rho_q}}$$

where f_0 is the unloaded resonance frequency, μ_q the shear modulus, and ρ_q the density of the quartz crystal. Furthermore, effects due to viscoelasticity of the adsorbed mass may occur, for example, during cell spreading. It is therefore essential to measure additional parameters, such as the maximal oscillation amplitude A_0 and the transient decay time constant τ. The maximal oscillation amplitude is the quartz amplitude that is reached after a 3-ms excitation with an oscillation frequency at the quartz resonance frequency. It reflects energy losses arising during excitation of the quartz crystal. It decreases with an increase of the viscosity–elasticity ratio of the adsorbed mass. The decay time constant τ, which corresponds to the ratio of mass over the energy losses, decreases with a more viscous adlayer. Finally a frequency decrease corresponds either to an increase of adsorbed mass in the case of a thin and rigid adlayer, and/or to a softening of the adlayer, since it has been shown that the sensitivity in frequency increases for softer adlayers [48]. The QCM used here including the measured parameters, the physical properties, and the equivalent circuit model have been described in more detail elsewhere [37]. Briefly, under water loading a resolution of f±2 Hz, A_0±50 a.u. (arbitrary units), and τ±1.4×10^{-6} s is obtained with 10-MHz crystals at 25±0.1 °C. Under vacuum the resolution is much better with f±0.03 Hz, A_0±3 a.u., and τ±1.5×10^{-8} s. Using the Sauerbrey relation, this corresponds to changes in surface mass density of m±9 ng cm^{-2} in liquid and m±0.135 ng cm^{-2} under vacuum.

Before each experiment the crystals were sterilized with ethanol and passed briefly over a flame. Experiments were performed at a constant temperature of 37±0.1 °C in order to obtain long-term stability and reproducibility of results. Moreover each solution was adjusted to 37 °C before introduction to the liquid cell to avoid changes in liquid density and viscosity. Before drug addition, the quartz surface was rinsed with a mixture of RPMI+x% DMSO, where x represents the drug dilution factor.

The evaporated Au electrodes were smooth. The small one had a diameter of 5 mm and the other one was in contact with liquid and covered completely the quartz surface [49]. The quartz crystal was entrapped between two plexiglas pieces sealed with VITON O-rings with inner diameter of 8 mm. The volume of the reaction chamber with the quartz crystal was 80 µL. Solutions were injected with a syringe via a closed tubing system, which prevented evaporation. The injection process lasted less than 5 s, and after injection no flow was maintained in the reaction chamber. Considering that the sensitive area corresponded to the smaller electrode, 3.12% of the total given *cell concentration* attached and spread out in this region.

Results and discussion

Cell attachment and spreading

We first studied the attachment of cultured human lung epithelial A549 cells to the Au electrode of QCM. The

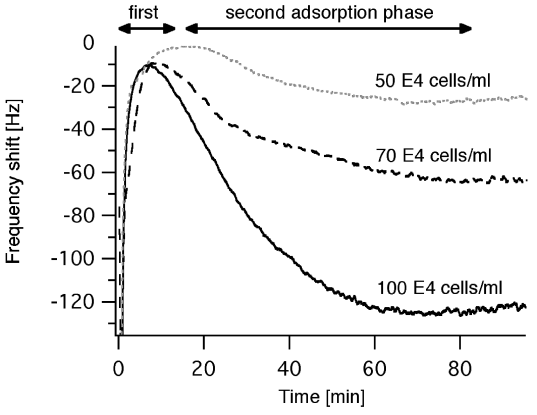

Fig 1 Adsorption of A549 cells at different concentrations. Larger frequency shifts were measured at larger cell concentrations

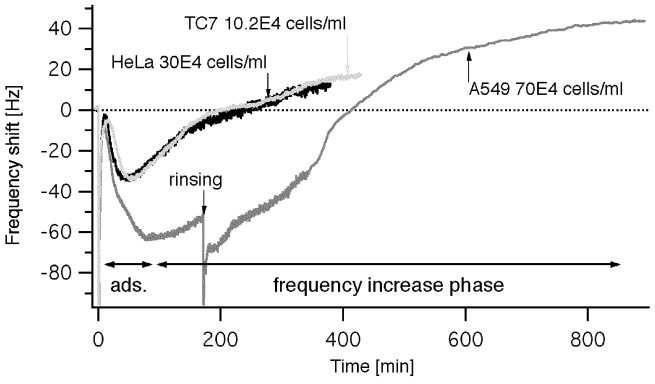

Fig. 2 Attachment and spreading of different cells at different concentrations. For long times (t>400 min) the frequency saturates above the frequency before cell injection. This frequency shift is observed for all investigated cell lines and is roughly proportional to the frequency shift at the end of the adsorption phase. After 180 min, the QCM surface containing A549 was rinsed (*arrow*) and the frequency continued to increase, indicating that the frequency increase was independent of media components that may be released during the adsorption phases

thickness sensitivity of our QCM under water loading at 37 °C was about 180 nm above the electrode surface [27]. All observed frequency variations were much smaller than the frequency shifts measured between the quartz exposed to air and solution, which was about 2 kHz. Before each experiment the quartz was equilibrated with growth medium lacking cells. Freshly trypsinized cells were injected onto the QCM in growth medium. Since the solutions had similar viscosities, frequency shifts were assigned to the response of cells attached on the crystal.

Figure 1 represents the frequency shifts measured during the attachment and spreading of A549 cells up to 80 min after injection. The frequency decreased dramatically during the first 40 s reaching levels between –187 Hz and –284 Hz. We attributed the first frequency changes to the injection process, that is, to the pressure difference during injection (see also Fig. 4, and ref. [37]). During the next 10–16 min, pressure on the quartz surface progressively decreased and accordingly, the frequency increased to levels between Δf=–2 Hz and Δf=–10 Hz (Fig. 1). Similar observations occur with protein adsorption, where the subsequent equilibration time is, however, much shorter (less than 1 min) [50]. It is not clear whether the quartz response in this first phase contained other signatures than that of the injection induced disturbance and the onset of cell adsorption. In the subsequent so-called second adsorption phase, the resonance frequency decreased. This was assigned to cells adhering to the solid substratum, as concluded from independent experiments performed on glass coverslips mounted on an inverted microscope equipped with phase contrast optics (data not shown). The maximal frequency shifts were roughly proportional to the cell concentration and typically lasted until about 80 min post-injection. Similar results have been obtained with other cell lines [30, 51]. At the end of the second adsorption phase, A549 cells induced larger frequency shifts at higher concentrations (Δf_2=–64 Hz with 70×10^4 cells mL^{-1} compared to Δf_2=–33 Hz with 30×10^4 HeLa cells mL^{-1}; see Fig. 2). The duration of the second adsorption phase was also cell type dependent, lasting 80 min for A549 and 50 min for HeLa and TC7 cells.

Surprisingly, we found that the frequency steadily increased afterwards (Fig. 2). This was observed with three different cell lines, the human epithelial HeLa and A549 cells and the African Green Monkey epithelial cells TC7. In all cases, the frequency passed the initial frequency measured before cell injection and at the beginning of the second adsorption phase. The magnitude and the kinetics of frequency shifts were concentration and cell type dependent, as similar frequency shifts were measured with HeLa and TC7 cells, albeit at different cell concentrations (30×10^4 cells mL^{-1} and 10.2×10^4 cells mL^{-1}, respectively). Positive frequency shifts Δf_{final}=+14 Hz were measured after 378 min for HeLa and TC7 and Δf_{final}=+43 Hz after 896 min for A549 cells. Similar frequency increases had previously been measured with neutrophils deposited on HSA-coated polystyrene [35] and with various cultured cells, but the nature of the increase is unknown [30, 51]. From our measurements it appeared that Δf_{final} was roughly proportional to Δf_2 (i.e., the number of adhered cells). Rinsing of the surface with growth medium at 175 min (see arrow in Fig. 2) did not disturb the frequency increase. Likewise, stopping the quartz excitation for several hours had no effect on the rate of frequency shift, indicating that the quartz oscillation per se was not responsible for the increase of frequency (data not shown).

To test whether cell desorption occurred during the frequency upshift we analyzed the QCM surface by light microscopy (see Fig. 3). Inspection by phase contrast microscopy indicated that 50% of the quartz surface was covered with A549 cells at 896 min post-injection (Fig. 3A). Fluorescence microscopy of HeLa or TC7 cells on the quartz electrode at 378 min or 429 min post injection identified actin filaments including focal contacts (arrows in Fig. 3B and C) at the cell periphery and across the cytoplasm indicative of cell spreading. In these cases the surface coverage was about 70% for HeLa and 60% for TC7 cells. It

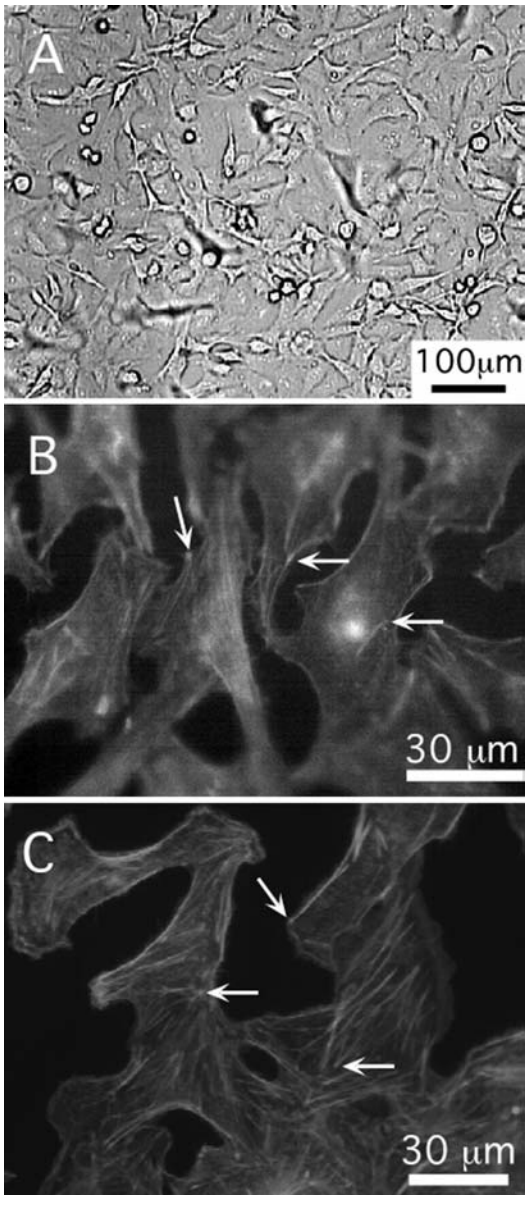

Fig 3A–C Microscopy analyses of the quartz surface after cell spreading when positive frequency shifts were measured. For each cell type the surface was covered with living cells indicating that no cell desorption during frequency upshifts were monitored: **A** phase contrast measurement directly above the QCM surface covered with spread out A549 cells seeded at 70×10^4 cells mL^{-1}, 896 min post-injection. **B** Phalloidin-FITC staining HeLa actin filaments (30×10^4 cells mL^{-1}), 378 min post-injection. *Arrows* point on actin complexes, suggestive of focal complexes or focal contacts linking the actin cytoskeleton to the extracellular substratum [52]. **C** Phalloidin-TR staining of TC7 (10.2×10^4 cells mL^{-1}), 429 min post-injection

is known that during adsorption, adherent cells establish tight focal contacts linking the actin cytoskeleton through receptors to the substratum [52]. The rest of the ventral cell surface is often distantly located from the substratum [53]. It is thus likely that only a fraction of the adsorbed cell mass is detected with the QCM measurements. However, since the frequency shifts depended not only on the surface coverage but also on the cell type, we suggest that intrinsic mechanical properties of individual cell types were also reflected in the QCM response. Most likely, the frequency increase was not due to cell desorption or QCM induced artifacts. Rather, it may have been an indication for the breakdown of the Sauerbrey equation, i.e., that the cells might alter their viscoelastic properties.

Maximal amplitude and decay time constant reveal changes of cell stiffness

To investigate the underlying nature of the frequency upshifts after cell adsorption we have also measured the decay time constant τ and the maximum oscillation amplitude A_0; τ and A_0 relate the stiffness of the adsorbed mass to energy losses [37]. A decrease of τ corresponds to a decrease of mass density and/or an increase of viscosity and a decrease of amplitude is induced by an increase of the viscosity–elasticity ratio of the adlayer as suggested earlier [37]. Kanazawa's equation indicates that frequency shifts can occur by modifying the liquid properties, such as the viscosity and density, in the absence of cell desorption [29]. In our experiments, the properties of the extracellular fluids remained largely constant during and after the introduction of the cells and we assumed that the extracellular matrix properties did not change drastically during our observations. Upon cell injection τ and A_0 decreased drastically from $A_0\approx6{,}000$ a.u. and $\tau\approx3{,}000\times10^{-6}$ s during the first and second initial "adsorption phases" (Fig. 4). This corresponded to an increase of dissipated energy per adsorbed mass and to energy loss. Energy loss can, for example, arise due to slipping of cells over the surface. Accordingly, the formation of the focal points linking the cells to the substratum is a highly dynamic process [54]. In addition the cytoplasm may not act as a standard solution in contact with the electrode surface because it is limited by the plasma membrane with dynamic biophysical and mechanical properties. During the "frequency increase phase" after about 60 min (brighter color in Fig. 4) the maximal amplitude decreased gently and stabilized at ΔA_0=–2,590 a.u. at about 200 min. In contrast, the decay time constant presented a minimum at 140 min post-injection and then slightly increased to -510×10^{-6} s at 378 min, similar to the value at the end of the second adsorption phase.

We then plotted ΔA_0 as a function of $\Delta\tau$ and compared the data to mixtures of ethanol and water (Fig. 4D). The water–ethanol line represents changes in amplitude and decay time constant due to modifications of solution properties. In this case both parameters are inversely proportional to the product of the liquid viscosity and density [37]. Clearly, the ratio of $\Delta A_0/\Delta\tau$ for HeLa cells was not constant, unlike the water–ethanol line. A similar behavior was observed with TC7 and A549 (see Fig. 5). Since all the ΔA_0 versus $\Delta\tau$ plots were below the water–ethanol line, energy dissipation by adsorbed cells was measured. During the first 50–80 min after introduction of the cell suspension to the QCM, ΔA_0 was a linear function of $\Delta\tau$

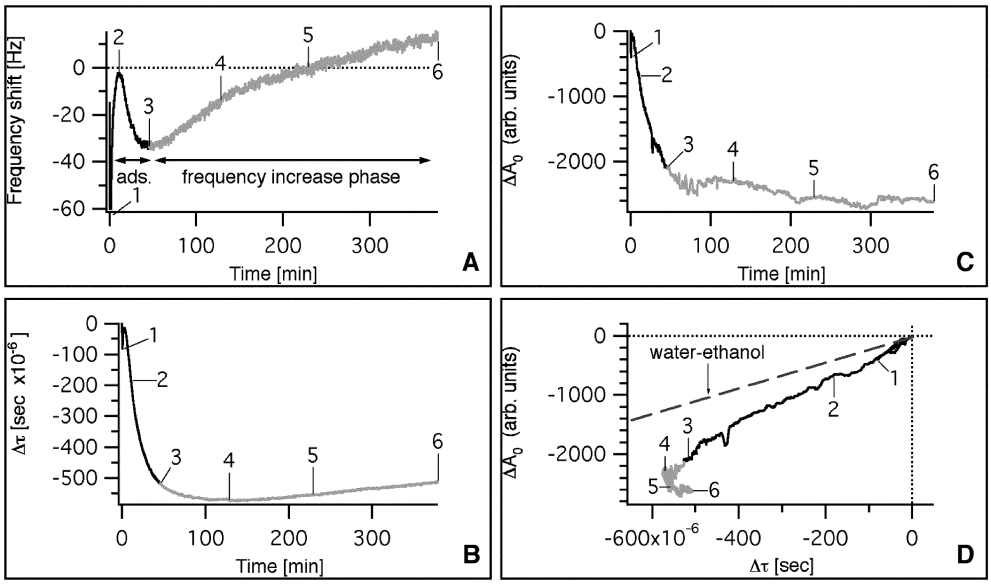

Fig 4A–D Frequency (**A**) (data taken from Fig. 2 for comparison), decay time constant (**B**) and amplitude (**C**) kinetics during HeLa attachment and spreading. **D** Maximal oscillation amplitude shift versus decay time constant shift including the water–ethanol line. The "frequency increase phase" is represented with a *brighter color* and reference time points are indicated by *numbers* (*1–6*)

and the curve nearly followed the water–ethanol line. The slope remained constant, independent of the cell type and the concentration in the range of 50–100×10^4 cells mL^{-1} (data not shown). Similar to $\Delta\tau$, ΔA_0 decreased during the first 40 s due to the injection process and increased thereafter following a similar slope. After this, ΔA_0 and $\Delta\tau$ decreased linearly for all cell types following the same slope as during the first 40 s. Nevertheless, the slopes were different for each cell type, that is, the largest slope was found with A549 and the smallest one with TC7 cells. Since A_0 decreases with an increase of energy loss, and τ decreases with a decrease of the ratio of adsorbed mass over energy loss, the A549 cells dissipated less energy per adsorbed mass than HeLa, which dissipated less energy than TC7 cells. Most likely the A549 cells were the stiffest cells followed by the HeLa and the TC7 cells. In accordance with this interpretation, the frequency kinetics were similar for HeLa and TC7 cells, albeit the concentration and surface coverage of TC7 cells were smaller than those of HeLa cells (Fig. 2). This was most likely due to the decreased QCM sensitivity in frequency with increased stiffness of adsorbed material [48].

During the phase of frequency increase after about 80 min (brighter color in Fig. 5) the behavior of the ΔA_0 versus $\Delta\tau$ curves was no longer linear. In the case of HeLa and TC7 cells, τ reached a minimal value and slightly increased thereafter. In this last phase A_0 remained constant. This phenomenon was particularly obvious when the quartz surface was rinsed (in the case of A459 cells). Then A_0 remained constant and τ increased (turning point, dashed arrow in Fig. 5), which suggested stiffening of the attached cells.

In summary the decrease of frequency in the second adsorption phase correlated with the attachment of cells. During this phase, the maximum oscillation amplitude decreased linearly as a function of the decay time constant. Thereafter the frequency increased mainly due to stiffening of the attached cells.

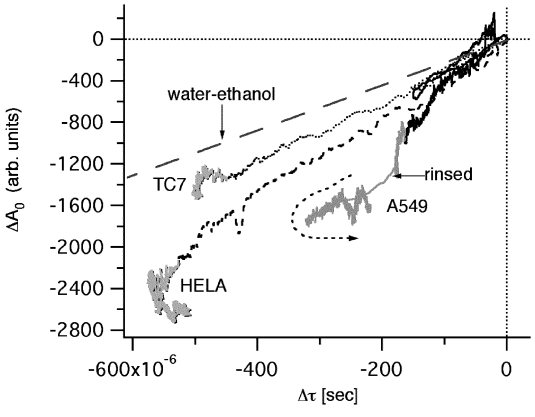

Fig 5 Maximal amplitude shift versus decay time constant shift during attachment of TC7 (10.2×10^4 cells mL^{-1}), HeLa (30×10^4 cells mL^{-1}, Fig. 4) and A549 cells (70×10^4 cells mL^{-1}) with water–ethanol curve as a reference. The "frequency increase phase" is represented with a *brighter color* for each cell type

Effects of cytoskeleton targeted drugs on f, τ, and A_0

During cell attachment and spreading focal contacts are developed, and filamentous actin is established in the cell cortex [53, 55]. In addition, actin and microtubule filaments are present in the cell periphery and across the cytoplasm yielding a cell-type-specific shape. The third type of cytoskeletal element, the intermediate filaments, are thought to be passively regulated subsequent to changes of the actin and microtubule filaments. To test if the variations of f, τ, and A_0 were due to cell alterations of the cytoskeleton inducing viscosity changes, we treated the attached cells with actin and microtubule inhibitors. As indicated by confocal laser scanning microscopy of chemically fixed A549 cells, the F-actin stabilizing drug jasplakinolide (Jas) prevented F-actin staining with the intercalating drug phalloidin indicative of F-actin stabilization

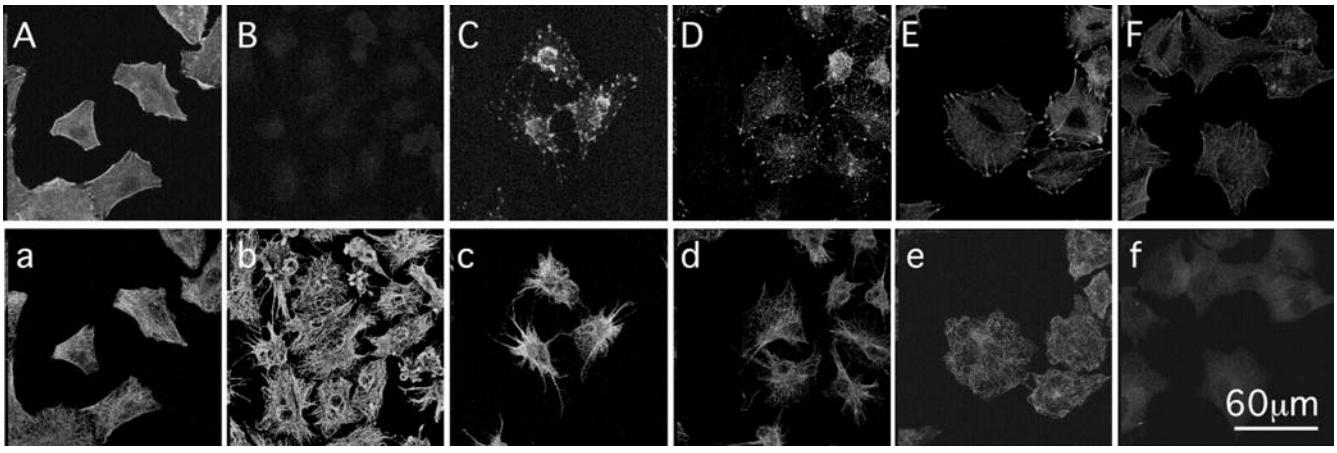

Fig 6Aa–Ff Confocal images of A549 cells treated with actin and microtubule inhibitors on glass coverslips stained for filamentous actin with phalloidin-FITC (*top*) and for microtubules using specific antibodies (*bottom*). The cytoskeleton of untreated A549 cells (**A** and **a**) was disturbed with Jas (**B** and **b**), CD (**C** and **c**), LatB (**D** and **d**), Taxol (**E** and **e**), or Noc (**F** and **f**). The scale in *f* is the same for all images. Projections of the confocal sections across the entire cells are shown

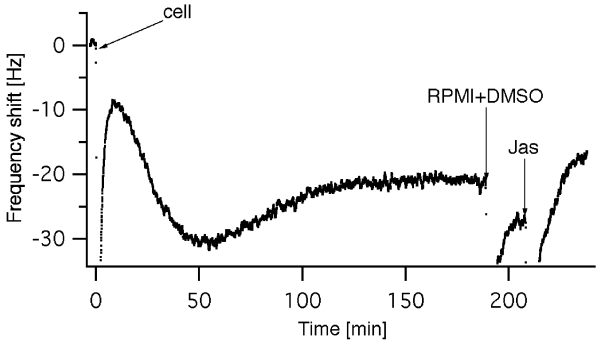

Fig 7 Frequency changes of attached A549 cells treated with Jas. The QCM surface was first rinsed with medium+DMSO, and then with medium plus Jas in DMSO (*arrows*)

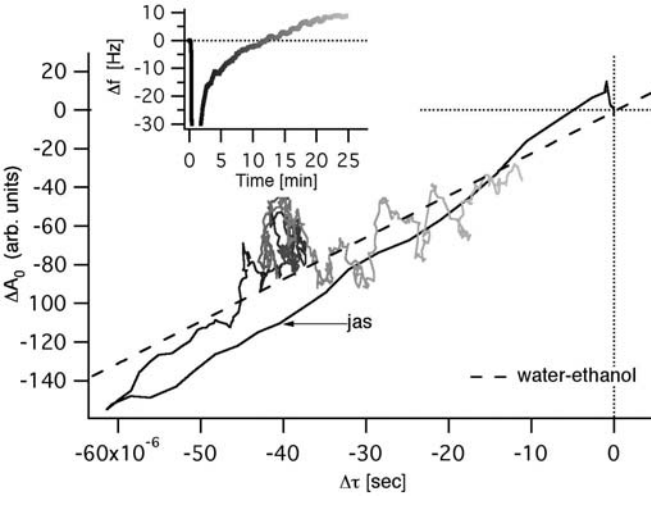

Fig 8 Increase of filamentous actin of Jas-treated A549 cells correlates with positive frequency shifts and ΔA_0 versus $\Delta\tau$ curve is indicative of cell stiffening. *Inset* Δf versus time upon Jas addition at 0 min

[39] (Fig. 6). The F-actin depolymerizing drugs cytochalasin D (CD) [46] and latrunculin B (LatB) led to F-actin fragmentation and cell contraction [44] (Fig. 6). The treatment of cells with the microtubule stabilizing drug paclitaxel (Taxol) resulted in microtubule aggregation [47], and nocodazole (Noc) promoted the depolymerization of microtubules, as expected [56]. Observation of drug effect on cytoskeleton was limited to 30 min, since their action at larger timescale and at high concentration is not well known.

We recorded the changes of f, A_0, and τ for attached A549 cells treated with Jas. Figure 7 presents a complete experiment including the two first "adsorption phases" and the "frequency increase phase". Before the introduction of Jas at 208 min, the quartz surface was rinsed with growth medium containing a similar concentration of the solvent dimethylsulfoxide (DMSO). This induced a small frequency decrease due to altered liquid properties. Importantly, however, DMSO-containing medium had a similar viscosity as the drug-containing medium. The addition of Jas induced a rapid frequency increase compared to non-treated cells or cells treated with medium+DMSO alone (see Fig. 7). At 25 min after the application of Jas, the Δf was at +9 Hz (Fig. 8, inset). Parallel experiments performed on coverslips showed no signs of cell desorption after 30 min of Jas treatment (Fig. 6B,b). We next plotted ΔA_0 versus $\Delta\tau$ for Jas-treated cells (Fig. 8). During the first 40 s the maximal amplitude A_0 and the decay time constant τ decreased and thereafter increased, similar to what was measured after the introduction of the cell suspension to neat quartz in the absence of drugs. Cells were probably slightly disturbed by the solution exchange process.

During the next 15 min, the maximal amplitude and the decay time constant remained constant under Jas treatment, ΔA_0=–70 a.u. and $\Delta\tau$=–40×10^{-6} s. It has been shown that for viscoelastic systems, such as cells, an increase of viscosity and viscosity–elasticity ratio can induce an increase of frequency [48]. The cell viscosity–elasticity ra-

tio had therefore to increase, inducing a positive frequency shift Δf=+4 Hz. Thereafter, the frequency continued to increase to about Δf=+9 Hz. Similarly $\Delta\tau$ increased to about -10×10^{-6} s and ΔA_0 versus $\Delta\tau$ slightly increased following the water–ethanol line. This phase indicated a stiffening of the cells that is consistent with the known cell biological action of Jas, which increases the F-actin stability and lowers the turnover of monomers [41].

We next treated the A549 cells attached to the QCM surface with the actin-depolymerizing drugs CD or LatB. The effects of CD and LatB on A_0 and τ were different from those observed with Jas. The decay time constant and the maximal amplitude increased to about $\Delta\tau$=+150×10^{-6} s and ΔA_0=+400 a.u. in 25 min, indicative of a viscosity decrease or cell desorption. The latter was confirmed by confocal light microscopy indicating that CD led to cell retractions due to the loss of filamentous actin (Fig. 6C, c). This suggested that QCM detected mainly cell detachment rather than viscosity/elasticity changes upon actin depolymerization, consistent with direct viscosity measurements [57, 58, 59]. Accordingly, the frequency increased by Δf=+11 Hz upon CD treatment (inset Fig. 9). Similar results have been obtained by others with Madine–Darby–Canine Kidney cells, using a steady state technique, measuring a decrease of resistance and inductance corresponding to a decrease of energy loss and mass desorption [32]. In contrast to CD-treated cells, the frequency decreased continuously under LatB treatment, reaching Δf=–32 Hz after 25 min (inset Fig. 9), in comparison to Δf_2=–23 Hz at the end of the second adsorption phase. Parallel experiments showed no signs of cell desorption (Fig. 6D, d). Therefore, the cell stiffness decreased under LatB treatment, increasing the quartz sensitivity in frequency.

We next treated attached A549 cells with Taxol and Noc. Taxol promotes microtubule stabilization by binding to the taxane binding site on beta tubulin [60], and Noc

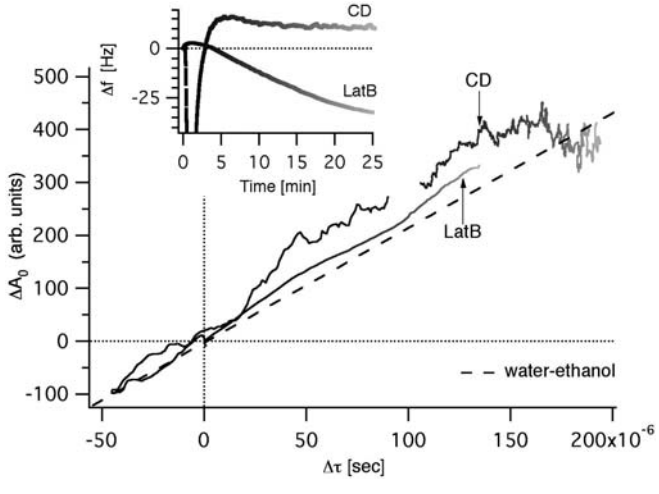

Fig 9 Depolymerization of actin filaments of A549 cells with CD and LatB drugs. *Inset* frequency shift versus time under CD and LatB treatment

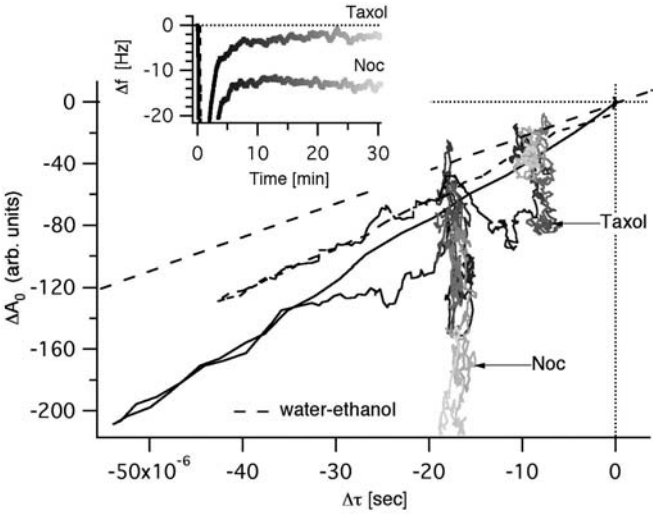

Fig 10 Polymerization of microtubules with Taxol and depolymerization with Noc. *Inset* frequency shift versus time under Taxol and Noc treatment

leads to microtubule depolymerization due to inhibition of tubulin incorporation [61]. As indicated in Fig. 10, Taxol induced no additional change in frequency (Δf=–2 Hz) in comparison to the maximal frequency shift Δf_2=–30 Hz at the end of the second adsorption phase. The ΔA_0 versus $\Delta\tau$ curves in Fig. 10 did not follow the water–ethanol line but remained below it, corresponding to mass adsorption with modification of the viscoelastic properties of the attached cells. The small ΔA_0=–40 a.u. and $\Delta\tau$=-8×10^{-6} s decreases corresponded to an insignificant increase of the cell viscosity, which was in accordance to measurements performed by others [57]. Parallel experiments showed no significant changes of the actin state, but microtubules were aggregated and the cell area seen in projection appeared to be increased (Fig. 6E, e). Therefore the small decrease of frequency might be due to increased cell spreading.

Depolymerization of microtubules was achieved by Noc treatment. After the successive decrease and increase of the maximal amplitude and of the decay time constant during the first 6 min (see Fig. 10), $\Delta\tau$ remained constant at -18×10^{-6} s and the maximal amplitude shift decreased from –80 a.u. to –210 a.u. in 30 min. During this period the frequency remained constant at Δf=–14 Hz and the parallel microscopy measurements showed that cell spreading somewhat increased in the presence of Noc (Fig. 6F, f), similar to Taxol. Therefore cell spreading and stiffness decrease of the attached cells most likely contributed to the frequency decrease. This in turn increased the sensitivity of frequency measurements. These results were consistent with an earlier report showing that Noc decreased the cell viscosity [57]. Another study also measured an initial decrease of frequency, which then increased during attachment and spreading [30], similar to our results. This study measured a frequency decrease upon treating attached endothelial cells with Noc. However the results

were interpreted as a restoration of rounded cell shape. The difference to our study may be different cell lines and cell confluences or unknown parameters. In any case, our results clearly indicate that QCM can detect modifications of the actin and microtubule polymerization state of cells attached to a solid substratum.

Conclusion

The QCM technique can be used to study the kinetics of adsorption and spreading of cells to a solid substratum. A key prerequisite to determine viscoelastic properties of the interface between the cells and the substratum is to simultaneously determine complementary parameters such as the frequency f, the maximal oscillation amplitude A_0, and the decay time constant τ. Our results show that the frequency measured during the initial 15 min of cell attachment reflects effects of the cell injection process. The effects are unspecific and largely due to pressure differences due to injection. During the second adsorption phase up to 80 min post-injection, the frequency decreased mainly due to cell attachment and spreading, firmly attaching to the QCM surface. After 80 min, the frequency increased for several hours and even passed the initial value, so that positive frequency shifts were measured. Optical measurements confirmed that the surface of the quartz crystal was covered with cells and that no obvious cell desorption occurred during this phase. ΔA_0 and $\Delta\tau$ measurements indicated that the frequency increase was mainly due to increased cell stiffness, which in turn affected the sensitivity of the frequency measurement. This was confirmed by treating the attached cells with agents affecting the polymerization state of actin and microtubule filaments. Positive frequency shifts were measured when the stiffness of the attached cells increased and/or when cell desorption occurred. Negative frequency shifts arose when cells became softer and/or the projection area of attached cells increased. It is, however, possible that additional factors influence the quartz response. For example, the contacts between the quartz electrode and the ventral side of the cells are not continuous but separated by cavities filled with extracellular medium. It is currently unknown if the QCM responds to local changes of the extracellular medium present in these cavities. To the best of our knowledge, no theoretical models have been developed for such nonhomogeneous cases. Nevertheless, it is obvious that any modification of the liquid between the cell and the solid surface likely contributes to the quartz response. The penetration depth of the damped wave coupled to the quartz can be influenced by the viscosity, stiffness, and shape of attached cells, which in turn affects the QCM frequency. Further experiments with systems presenting phase transitions have to address the influence of these different parameters.

Acknowledgments We gratefully acknowledge Laurent Spicher and Francis Bourqui for their work in the building of the QCM. We also thank Bianca Saam and Karin Boucke for the cell culture and Dr Robert Stidwill for the confocal images. This work was supported by the Dr h.c. Robert Mathys Stiftung (RMS) Foundation and the Swiss National Science Foundation (TopNano21).

References

1. Walpita D, Hay E (2002) Nat Rev Mol Cell Biol 3(2):137–141
2. McIntosh JR, Grishchuk EL, West RR (2002) Annu Rev Cell Dev Biol 18:193–219
3. Goldstein LS, Philp AV (1999) Annu Rev Cell Dev Biol 15: 141–183
4. Huang S, Ingber DE (1999) Nat Cell Biol 1(5):E131–138
5. Huang S, Ingber DE (2000) Exp Cell Res 261(1):91–103
6. Barbee KA, Davies PF, Ratneshwar L (1994) Circ Res 74:163–171
7. PouratiJ, Maniotis A, Spiegel D, Schaffer JL, Butler JP, Fredberg JJ, Ingber DE, Stamenovic D, Wang N (1998) Am J Physiol 274:C1283–C1289
8. Allen RD (1985) Ann Rev Biophys Biophys Chem 14:265
9. Chamberlain C, Hahn KM (2000) Traffic 1(10):755–762
10. Wang N, Tolic-Norrelykke IM, Chen J, Mijailovich SM, Butler JP, Fredberg JJ, Stamenovic D (2002) Am J Physiol Cell Physiol 282(3):C606–C616
11. Puig-De-Morales M, Grabulosa M, Alcaraz J, Mullol J, Maksym GN, Fredberg JJ, Navajas D (2001) J Appl Physiol 91(3):1152–1159
12. Berrios JC, Schroeder MA, Hubmayr RD (2001) J Appl Physiol 91(1):65–73
13. Wang Q, Chiang ET, Lim M, Lai J, Rogers R, Janmey PA, Shwpro D, Doerschuk CM (2001) Blood 97(3):660–668
14. Bausch AR, Hellerer U, Essler M, Aepfelbacher M, Sackmann E (2001) Biophys J 80(6):2649–2657
15. Bausch AR, Ziemann F, Boulbitch AA, Jacobson K, Sackmann E (1998) Biophys J 75:2038–2049
16. Ziemann F, Rädler J, Sackmann E (1994) Biophys J 66:2210–2216
17. Kolega J (1986) J Cell Biol 102:1400–1411
18. Hochmuth RM, Waugh RE (1987) Annu Rev Physiol 49:209–219
19. Evans E, Yeung A (1989) Biophys J 56:151–160
20. Evans E, Berk D, Leung A (1991) Biophys J 59:838–848
21. Sung KLP, Kwan MK, Maldonado F, Akeson WH (1994) J Biomech Eng 116:237–242
22. Petermon NO, McConnaughey WB, Elson EL (1982) Proc Natl Acad Sci USA 79:5327–5331
23. Pastermank C, Wong S, Elson EL (1995) C Cell Biol 128: 355–361
24. Janshoff A, Galla H-J, Steinem C (2000) Angew Chem Int Ed 39:4004–4032
25. Jones JL, Meiure JP (1969) Anal Chem 41:484
26. Meiure JP, Jones JL (1969) Talanta 16:149–150
27. Sauerbrey G (1959) Z Phys 155:206–222
28. Nomura T, Iijima M (1981) Anal Chim Acta 131:97–102
29. Kanazawa KK, Gordon JG (1985) Anal Chem 57:1770–1771
30. Marx KA, Zhou T, Montrone A, Schulze H, Braunhut SJ (2001) Biosens Bioelectron 16:773–782
31. Zhou T, Marx KA, Warren M, Schulze H, Braunhut SJ (2000) Biotechnol Prog 16:268–277
32. Wegener J, Seebach J, Janshoff A, Galla H-J (2000) Biophys J 78:821–2833
33. Janshoff A, Wegener J, Sieber M, Galla H-J (1996) Eur Biophys J 25:93–103
34. Otto K, Elwing H, Hermansson M (1999) J Bacteriol 181(17): 5210–5218
35. Nimeri G, Fredriksson C, Elwing H, Liu L, Rodahl M, Kasemo B (1998) Coll Surf B Biointerfaces 11:255–264
36. Fredriksson C, Khilman S, Kasemo B (1998) J Mater Sci Mater Med 9:785–788
37. Galli Marxer C, Collaud Coen M, Bissig H, Greber UF, Schlapbach L (2003) Anal Bioanal Chem (in press) DOI 10.1007/s00216-003-2081-0

38. Suomalainen M, Nakano MY, Keller S, Boucke K, Stidwill RP, Greber UF (1999) J Cell Biol 144:657–672
39. Holzinger A (2001) Methods Mol Biol 161:109–120
40. Bubb MR, Spector I, Beyer BB, Fosen KM (2000) J Biol Chem 275:5163–5170
41. Bubb MR, Senderwicz AM, Sausville EA, Duncan KL, Korn ED (1994) J Biol Chem 269:14869–14871
42. Nakano MY, Boucke K, Suomalainen M, Stidwill RP, Greber UF (2000) J Virol 74(15):7085–7095
43. Coue M, Brenner SL, Spector I, Korn ED (1987) FEBS Lett 213:316–318
44. Spector I, Shochet NR, Blasberger D, Kashman Y (1989) Cell Motil Cytoskel 13:127–144
45. Urbanik E, Ware BR (1989) Arch Biochem Biophys 269:181–187
46. Cooper JA (1987) J Cell Biol 105:1473–1478
47. Schiff PB, Fant J, Horwitz SB (1979) Nature 277:665–667
48. Kanazawa KK (1997) Faraday Discuss 107:77–90
49. Rodahl M, Höök F, Kasemo B (1996) Anal Chem 68:2219–2227
50. Galli Marxer C, Collaud Coen M, Schlapbach L (2003) J Colloid Interface Sci 261(2):291–298
51. Wegener J, Janshoff A, Galla H-J (1998) Eur Biophys J 28: 26–37
52. Geiger B, Bershadsky A (2001) Curr Opin Cell Biol 13(5): 584–592
53. Burridge K, Fath K, Kelly T, Nuckolls G, Turner C (1988) Annu Rev Cell Biol 4:487–525
54. Petit V, Thiery JP (2000) Biol Cell 92:477–494
55. Bereiter-Hahn J, Luck M, Miebach T, Stelzer HK, Voth M (1990) J Cell Sci 96(1):171–188
56. Hoebeke J, Van Nijen G, DeBrabender M (1976) Biochem Biophys Res Commun 69:319–324
57. Wang N (1998) Hypertension 32:162–165
58. Thoumine O, Cardoso O, Meister J-J (1999) Eur Biophys J 28:222–234
59. Wakatsuki T, Schwab B, Thompson NC, Elson EL (2001) J Cell Sci 114(5):1025–1036
60. Nogales E, Wolf SG, Downing KH (1998) Nature 391:199–203
61. Wilson L, Jordan MA (1994) Microtubules. Hyams and Lloyd, Wiley-Liss, pp 59–83